TRIBOLOGY OF COMPOSITE MATERIALS

J. Paulo Davim

Editor

TRIBOLOGY OF COMPOSITE MATERIALS

MATERIALS AND MANUFACTURING TECHNOLOGY

J. PAULO DAVIM - SERIES EDITOR –

UNIVERSITY OF AVEIRO,
AVEIRO, PORTUGAL

Tribology Research Advances

J. Paulo Davim (Editor)

2009. ISBN: 978-1-60692-885-1

Drilling of Composite Materials

J. Paulo Davim (Editor)

2009: ISBN: 978-1-60741-163-5 (Hardcover)

2009: ISBN: 978-1-60876-584-3 (E-book)

Artificial Intelligence in Manufacturing Research

J. Paulo Davim (Editor)

2010: ISBN: 978-1-60876-214-9 (Hardcover)

2010. ISBN: 978-1-61761-564-1 (E-book)

Metal Cutting: Research Advances

J. Paulo Davim (Editor)

2010. ISBN: 978-1-60876-207-1 (Hardcover)

2010. ISBN: 978-1-61122-573-0 (E-book)

Tribology of Composite Materials

J. Paulo Davim (Editor)

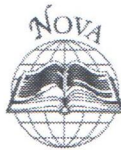2010. ISBN: 978-1-61668-319-1

Micro and Nanomanufacturing Research

J. Paulo Davim (Editor)

2010. ISBN: 978-1-61668-488-4

TRIBOLOGY OF COMPOSITE MATERIALS

J. PAULO DAVIM

EDITOR

CONTENTS

PREFACE

Recently, the use of composite materials has increased in various areas of science and technology due to their special properties, with applications in biomedical, aircraft, automotive, defence and aerospace, as well other advanced industries. Tribology is defined as the *"science and technology of interacting surfaces in relative motion"*. It includes the research and application of principles of friction, wear and lubrication. Recently, nanocomposites had been gaining ground. Frictional interactions in micro and nanocomponents are becoming increasingly important for the development of new products in several industries.

This book aims to provide the research and review studies on tribology of composite materials. The first chapter provide information on tribology of functionalised carbon nanofillers based polymer composites. Chapter 2 is focused on tribology of injection molded thermoplastic nanocomposites. Chapter 3 discuss tribology of composite materials with inorganic lubricants. Chapter 4 is focused on mechanical and tribological behaviors of nanometer Al_2O_3 and SiO_2 reinforced PEEK composites. Subsequently, the chapter 5 deal with the effects of matrix crystalline structure and molecular weight on the tribological behaviour of PEEK-based materials. Chapter 6 is focused on friction and wear of Al_2O_3-Ni composite. Chapter 7 discuss modelling and analysis on wear behaviour of metal matrix composites. Finally, the last chapter of this research book is focused on some aspects of tribology of glass-ceramic bonded composite materials.

The present research book can be used for final undergraduate engineering course (for example, materials, mechanical, physics, etc) or as a subject on tribology of composite materials at the postgraduate level. Also, this book can serve as a useful reference for academics, researchers, materials, mechanical and physics engineers, professional in related industries with composite materials.

The Editor acknowledges gratitude to Nova Publishers for this opportunity and for their professional support. Finally, I would like to thank all the chapter authors for their availability for this work.

J. Paulo Davim
Aveiro, Portugal
November 2009

Chapter 6

FRICTION AND WEAR OF AL$_2$O$_3$-NI COMPOSITE

Jinjun Lu[1,], Junhu Meng[1], Bin Liu[2], Jingbo Wang[1], and Shengrong Yang[1]*

1. State Key Laboratory of Solid Lubrication,
Lanzhou Institute of Chemical Physics,
Chinese Academy of Sciences, Lanzhou, P.R. China
2. School of Stomatology,
Lanzhou University, Lanzhou, PR China

ABSTRACT

Al$_2$O$_3$-Ni powders with different volume fraction of Ni were prepared by a three-step reduction method and then hot-pressed into Al$_2$O$_3$-Ni composites at elevated temperatures. Scanning electron microscopy observation on the microstructure of Al$_2$O$_3$-Ni composites indicated inter-type and intra-type of Ni particles. Considerable growth of Al$_2$O$_3$ grain and Ni grain was also observed. The addition of Ni resulted in reduced hardness while increased bending strength. Very limited improvement on the fracture toughness can be obtained only for composite with 15 vol.% Ni. Friction and wear of monolithic Al$_2$O$_3$ and Al$_2$O$_3$-Ni composites in sliding against a Si$_3$N$_4$ ball were investigated at room temperature in air. Results indicated that a transition from mild wear to severe wear was found for Al$_2$O$_3$/Si$_3$N$_4$ tribo-couple. There was no such a transition for Al$_2$O$_3$-Ni composites in sliding against a Si$_3$N$_4$ ball. At high loads, Al$_2$O$_3$-Ni composites exhibited much better wear resistance than that of monolithic Al$_2$O$_3$. Wear mechanism for monolithic Al$_2$O$_3$ in mild wear regime was asperity-scale failure while it was related to the formation and detachment of tribo-layer in severe wear regime. Worn surfaces of Al$_2$O$_3$-Ni composites at 3 N and 5 N were very smooth. At high loads, the formation and detachment of tribo-layer on the worn surfaces of Al$_2$O$_3$-Ni composites played very important roles in affecting the tribological behavior and wear mechanism.

---

[*] Corresponding author, E-mail: jjlu@lzb.ac.cn.

1. INTRODUCTION

Alumina (Al_2O_3) has been the focus of research and development in the past decades as tribo-material. Its tribological behaviors, e.g. friction and wear in sliding, erosion, fluids and high temperature [1-4] were extensively investigated. Study on effect of second phase on the mechanical property of Al_2O_3 was active in recent years. In addition, there were some interesting papers concerning the effect of second phase on tribological behavior [5].

Al_2O_3-based nanocomposites, e.g. Al_2O_3-Ni composite [6] and Al_2O_3-SiC composite [7-8] have attracted many attentions because of their excellent mechanical properties. In addition, the tribological behavior of Al_2O_3-SiC composite was investigated [8]. It is interesting to investigate the tribological behavior of Al_2O_3-metal composites [9-10], especially for composite reinforced by sub-micron or even nano metal particles. In this chapter, Al_2O_3 ceramics reinforced by submicron Ni particles were prepared. Their microstructure, mechanical strength and tribological behavior were investigated. Finally, wear mechanisms were discussed.

2. MATERIALS AND EXPERIMENTAL DETAILS

2.1. Materials

2.1.1. Preparation of Al_2O_3-Ni Composite Powder

The Ni/Al_2O_3 powders with different amounts of Ni (5%, 10% and 15% in volume fraction unless otherwise stated) were prepared by a three-step reduction method as shown in Figure 1. This strategy for preparation of Al_2O_3-Ni composite powder in this chapter has been widely adopted for the synthesis of oxide-supported metal catalyst, which enables successful synthesis of γ-Al_2O_3/Ni powder with Ni nanoparticles well-dispersed on the γ-Al_2O_3 support.

Firstly, α-Al_2O_3 powder (commercially available from China Building Materials Academy) with an average particle size of 0.36 μm and $Ni(NO_3)_2 \cdot 6H_2O$ powder (commercially available from Baiyin Chemical Reagent Factory, China) were mixed and ball-milled in the presence of ethanol for 24 h with agate balls (step 1). And then, the mixture was calcined at 450 °C in air in an oven and followed by another ball-milling process in ethanol for 24 h to break the agglomerate (step 2). The powder was reduced in dry hydrogen at 600 °C for 1 h (step 3).

The phases of products in each step were α-Al_2O_3 and $Ni(NO_3)_2 \cdot 6H_2O$ in Figure 2a (step 1), α-Al_2O_3 and NiO in Figure 2b (step 2), and α-Al_2O_3 and Ni in Figure 2c (step 3). The following reactions were proposed for steps 2 and 3, respectively:

$$2Ni(NO_3)_2 \cdot 6H_2O(s) \rightarrow 2NiO(s) + 4NO_2(g) + O_2(g) + 6H_2O(g) \tag{1}$$

$$NiO(s) + H_2(g) \rightarrow Ni(s) + H_2O(g) \tag{2}$$
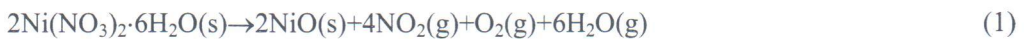
Spherical Ni particles (10 to 40 nm in diameter) were found to be well-dispersed on α-Al$_2$O$_3$ particles (Figure 3). The phase composition of the sintered body (Figure 2d) was the same as that of Al$_2$O$_3$/Ni composite powder in step 3 (Figure 2c).

```
┌─────────────────────────────────────┐
│   Al₂O₃+Ni(NO₃)₂.6H₂O                │
└─────────────────────────────────────┘
                  │
                  ▼
┌─────────────────────────────────────┐
│   Wet ball-milling in alcohol for 24 h │
└─────────────────────────────────────┘
                  │
                  ▼
┌─────────────────────────────────────┐
│      Filtering and drying            │
└─────────────────────────────────────┘
                  │
                  ▼
┌─────────────────────────────────────┐
│      Calcined at 500 °C              │
└─────────────────────────────────────┘
                  │
                  ▼
┌─────────────────────────────────────┐
│      Wet and dry ball-milling        │
└─────────────────────────────────────┘
                  │
                  ▼
┌─────────────────────────────────────┐
│      Reduction at 600 °C             │
└─────────────────────────────────────┘
                  │
                  ▼
┌─────────────────────────────────────┐
│        Hot pressing                  │
└─────────────────────────────────────┘
```
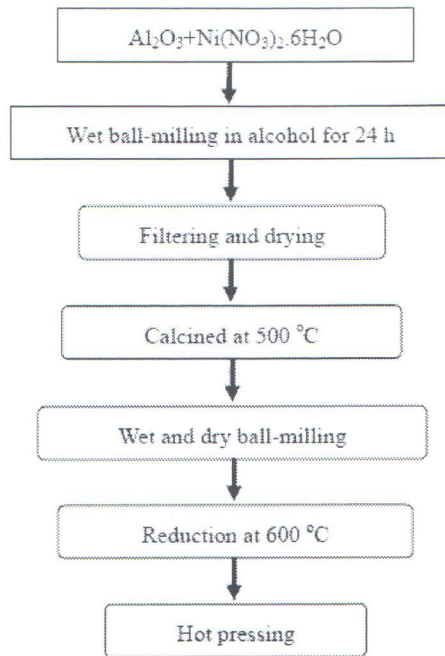
Figure 1. Schematic illustration of routine to prepare Al$_2$O$_3$-Ni composite powder and Al$_2$O$_3$-Ni composite.
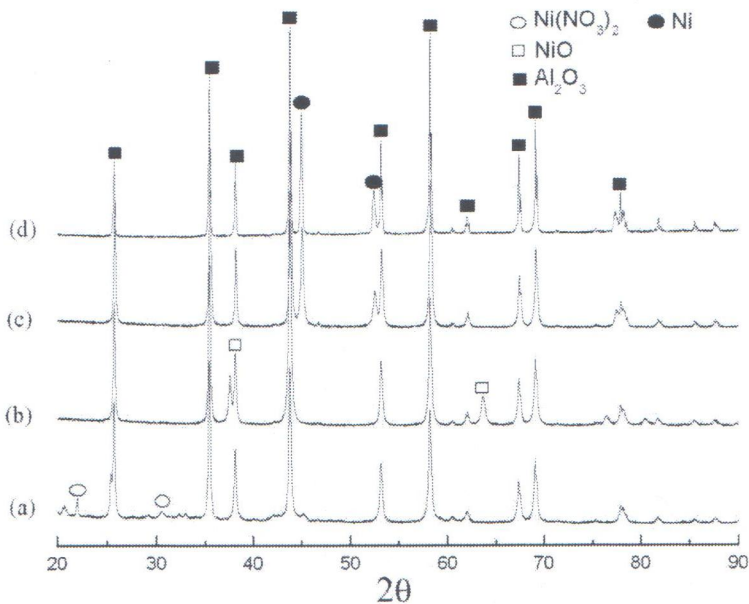

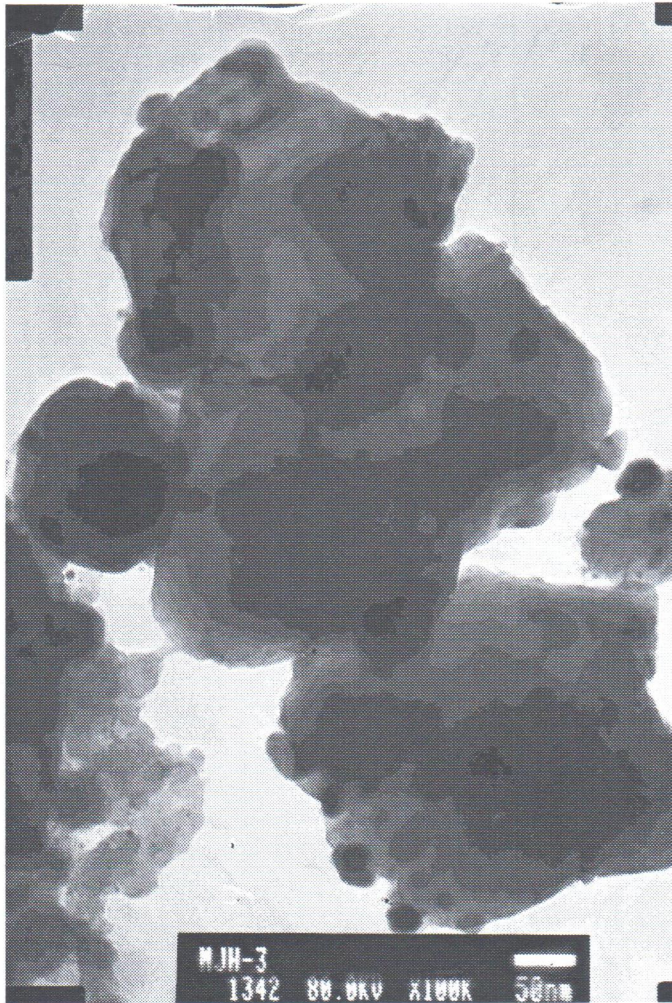Figure 2. XRD patterns of products of each step in Figure 1.

Figure 3. TEM micrograph of Al_2O_3-5%Ni composite powder.

2.1.2. Preparation and Microstructure of Al_2O_3-Ni Composite

After being crushed and sieved, the Al_2O_3-Ni composite powder was hot-pressed at 1400 °C to 1550 °C for 60 min under a pressure of 30 MPa in an argon atmosphere. The sintering temperature and schedule were optimized for Al_2O_3-Ni composites but is not the topic of this chapter. Monolithic Al_2O_3, as a reference sample, was hot-pressed at 1500 °C for 30 min. The average grain size d_{50} of monolithic Al_2O_3 was 10 μm.

The average size of Ni particles in Al_2O_3-Ni composite increased considerably to several hundred nanometers (Figure 4) compared with that of Ni particles in Al_2O_3-Ni composite powders (Figure 3) . Inter-type Ni particles as well as intra-type particles were found. Inter-type refers to particles located at the Al_2O_3/Al_2O_3 grain boundaries and the triple junctions while intra-type means particles located within Al_2O_3 grains.

Grain size d_{50} of Al_2O_3 in Figure 4a was ca. 2 μm. As the content of Ni increased, the grain sizes d_{50} of Al_2O_3 with 10% and 15% Ni decreased to be less than 1 μm. Therefore, it can be deduced that Ni particles effectively inhibited the growth of Al_2O_3 grains.
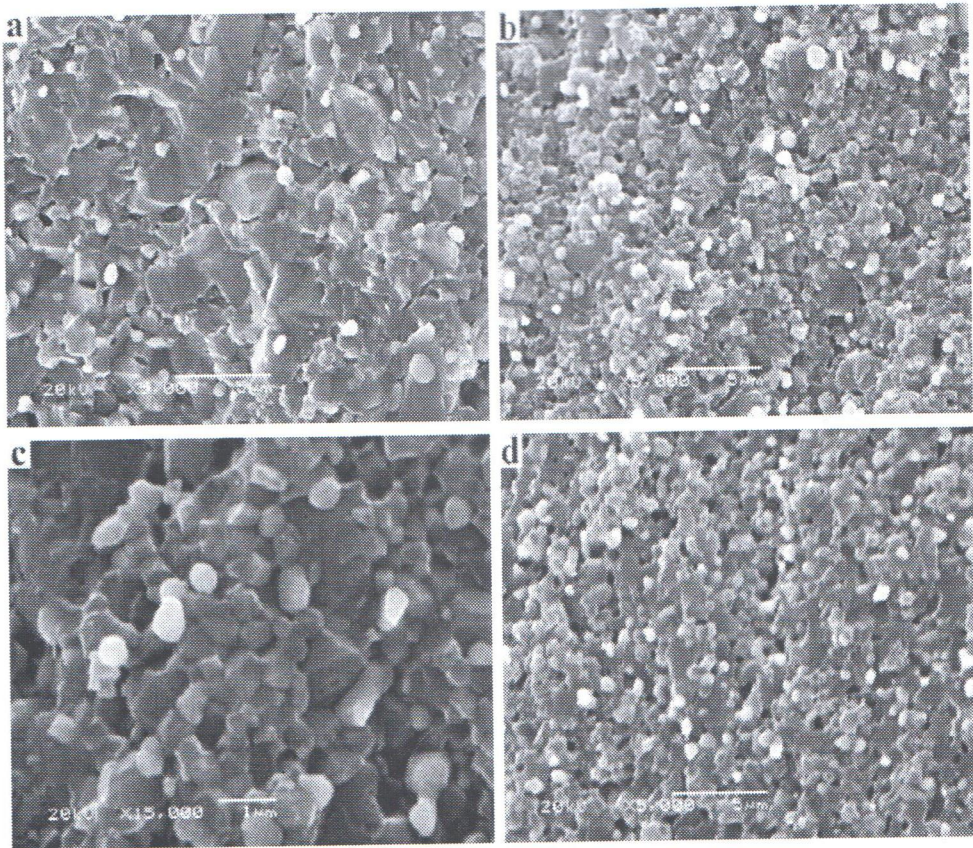
Figure 4. Fractured surfaces of (a) Al$_2$O$_3$-5%Ni composite, (b,c) Al$_2$O$_3$-10%Ni composite, and (d) Al$_2$O$_3$-15%Ni composite.

Table 1. Grain size and mechanical strengths of monolithic Al$_2$O$_3$ and Al$_2$O$_3$-Ni composite

Composition	Al$_2$O$_3$	Al$_2$O$_3$-5%Ni	Al$_2$O$_3$-10%Ni	Al$_2$O$_3$-15%Ni
Grain size of Al$_2$O$_3$ d50, μm	10	2	0.8	0.8
Hardness, GPa	17.40±0.85	16.00±0.53	15.53±0.44	13.84±0.22
Three-point bending strength, MPa	194.4±19.9	378.8±36.5	585.00±106.4	528.6±55.0
Fracture toughness, MPa m$_{1/2}$	3.60±0.30	3.37±0.16	3.37±0.13	4.38±0.16

Table 2. The physical and mechanical properties of Si$_3$N$_4$ ball from supplier

Density, g/cm^3	Vickers hardness, GPa	Fracture toughness, MPa m$^{1/2}$	Bending strength, MPa	Elasticity modulus, GPa
3.20~3.30	13~16	5.0~7.0	600~1000	300~320

2.1.3. Mechanical Property of Al₂O₃-Ni Composite

The hot-pressed samples were machined and polished for mechanical and tribological tests. The density of the samples was determined by Archimeds' principle using distilled water. All the samples were sintered to nearly full density. Rectangular beam samples ($3\times4\times40$ mm³) were used to measure the three-point bending strength with a span of 20 mm at a crosshead speed of 0.05 mm/min. Vickers hardness was measured using a load of 98 N and a dwell time of 5 s. Fracture toughness (K_{IC}) was obtained by the indentation method using the equation:

$$K_{IC} = P(\pi.b)^{-3/2}(tg\beta)^{-1} \tag{1}$$

where P is the load, b is the crack length and β is 68°.

Mechanical strengths of monolithic Al₂O₃ and Al₂O₃-Ni composite were listed in Table 1. The addition of Ni led to a reduction in hardness despite of much smaller grain size in Al₂O₃-Ni composites, as shown in Figure 4. According to Hall-Petch relationship, the hardness of fine-grain material is higher than that of coarse-grain material. This relationship has been experimentally supported in many studies. Ni is 'softer' than alumina and more easily plastically deformed. Then it is not surprising that the reduction in hardness can be attributed to Ni phase in the composite.

As seen in Table 1, the bending strength of Al₂O₃ can be markedly improved with the addition of Ni. Composite with 10% Ni had the highest bending strength. The initial idea of introducing Ni particle is to prompt the toughness of Al₂O₃. However, very limited improvement on the fracture toughness can be obtained only for composite with 15% Ni. There were no improvement in cases of Al₂O₃-5% Ni and Al₂O₃-10% Ni composites. According to Figure 4, Al₂O₃-Ni composites showed the mixed mode of transgranular and intergranular fractures.

2.2. Friction and Wear Test

The tribological tests were conducted on a reciprocating tribometer (UMT-2MT, USA) with a ball-on-disk configuration. The upper specimen was a commercially available Si₃N₄ ball with 3 mm in diameter (Shanghai Research Institute of Materials), and the lower specimen was an Al₂O₃-Ni composite disk with a size of 25 mm in diameter and 8 mm in thickness. An Al₂O₃ disk was used as a reference. The surface roughness (R_a) of Si₃N₄, Al₂O₃ and Al₂O₃-Ni composites was about 0.020 μm. The mechanical properties of Si₃N₄ balls are listed in Table 2. Prior to commencing a tribological test, the specimens were ultrasonically cleaned in an alcohol bath and allowed to dry. The test condition was as follow: a sliding speed of 1 m/s, a stroke of 5 mm and a sliding distance of 5400 m under different normal loads in the range of 3 to 20 N The measured relative humidity and ambient temperature were 30 to 40% and 25 °C, respectively. Wear volumes were calculated by measuring the worn volume of the ball and the area of wear track cross section on the disk, using an optical microscopy and a surface profilometry. The friction coefficients were recorded continuously during the test by a computer.

The worn surfaces of monolithic Al$_2$O$_3$, Al$_2$O$_3$-Ni composite and wear debris were analyzed on JSM-5600LV scanning electron microscopy (SEM) equipped with energy dispersive spectroscopy (EDS).

3. RESULTS AND DISCUSSION

3.1. Friction Coefficient

Figure 5 shows the friction coefficient of monolithic Al$_2$O$_3$ and Al$_2$O$_3$-Ni composites in sliding against Si$_3$N$_4$ under different loads. Friction coefficients of monolithic Al$_2$O$_3$ sliding against Si$_3$N$_4$ were in the range of 0.26 to 0.55. In case of Al$_2$O$_3$-5%Ni against Si$_3$N$_4$, friction coefficients were 0.60 at 3 N and around 0.40 at loads of 5 to 20 N. Friction coefficients of Al$_2$O$_3$-10% Ni and Al$_2$O$_3$-15% Ni against Si$_3$N$_4$ at 5 N and 10 N were higher than that of Al$_2$O$_3$-5% Ni composite.

3.2. Wear Rate

The wear rates of monolithic Al$_2$O$_3$ in Figure 6a indicated a transition from mild wear to severe wear as a function of load . The critical load for this transition was between 5 N and 10 N. Likewise, similar transition of wear was found for the counterpart Si$_3$N$_4$ (Figure 6b).

The wear rates of the three Al$_2$O$_3$-Ni composites at loads of 3 N and 5 N were higher than that of monolithic Al$_2$O$_3$ while the wear rates at loads of 10 N, 15 N and 20 N were much lower than that of monolithic Al$_2$O$_3$, see Figure 6. No transition from mild wear to severe wear was found for Al$_2$O$_3$-Ni composites at given loads.

In summary, Al$_2$O$_3$-Ni composites exhibited better wear resistance and higher critical load for transition from mild wear to severe wear than that of monolithic Al$_2$O$_3$.

3.3. Wear Mechanisms

3.3.1. Monolithic Al$_2$O$_3$

Wear mechanisms for monolithic Al$_2$O$_3$ sliding against Si$_3$N$_4$ in mild wear regime and severe wear regime will be discussed on two aspects, i.e. topography and chemical composition of worn surface of monolithic Al$_2$O$_3$ as well as topography of wear debris.

Figure 7 shows SEM micrographs of the worn surface of monolithic Al$_2$O$_3$ and corresponding wear debris at 3 N. The wear of monolithic Al$_2$O$_3$ at 3 N was so low that the cavities, which were the result of grain pulloff during grinding and polishing, still can be seen on the worn surface (Figs. 7a and 7b). The wear debris was agglomerates up to several hundreds of microns (Figure 7c) and actually very fine particle (Figure 7d). Most of them were less than 1 µm in size, which was much lower than the grain size of Al$_2$O$_3$. This means that grains were gradually removed in asperity-scale and corresponding wear was low. EDS result showed that no transfer and mechanical mixing occurred.
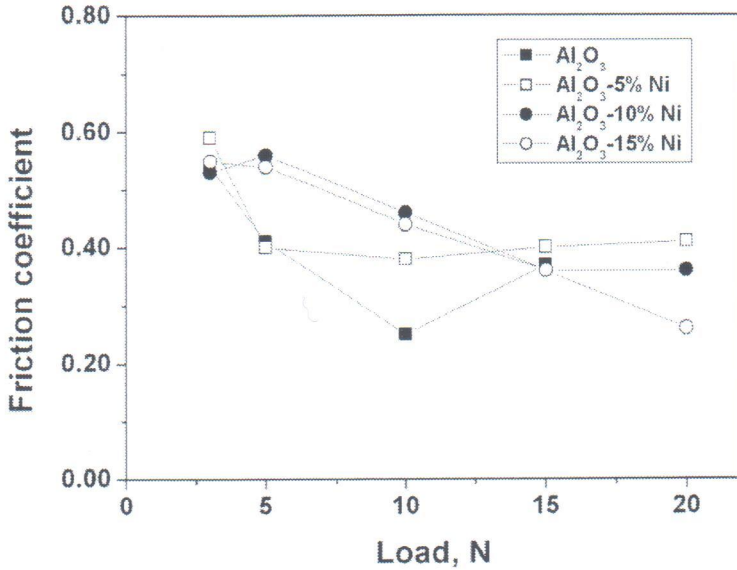
Figure 5. Friction coefficient of monolithic Al_2O_3 and Al_2O_3-Ni composites in sliding against Si_3N_4 under different loads.
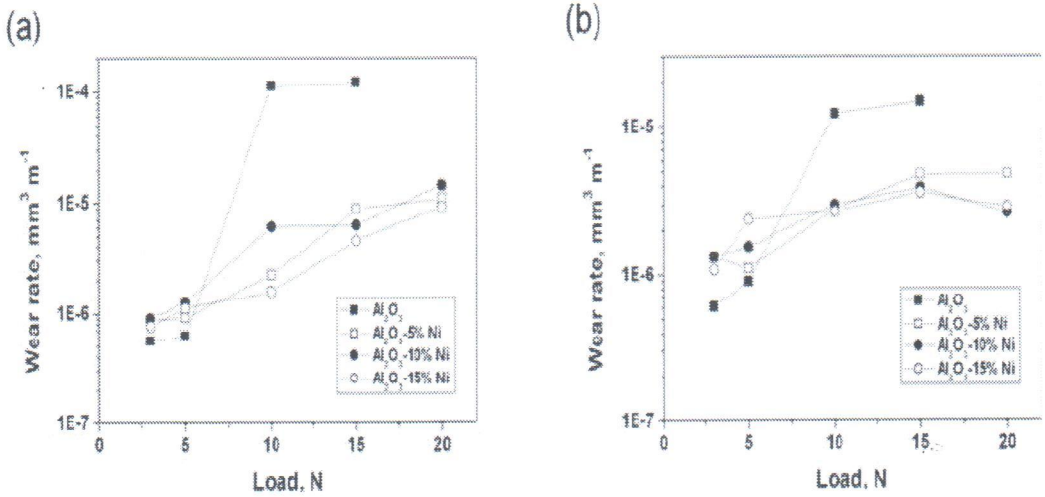

Figure 6. Wear rates of (a) monolithic Al_2O_3 and Al_2O_3-Ni composites and (b) Si_3N_4 as a function of normal load.

The topographies of the worn surfaces of monolithic Al_2O_3 at loads of 10 N (Figure 8a) and 15 N (Figure 8b) were totally different to that at 3 N and 5 N. The worn surfaces were characterized by two distinct areas: smooth area (tribo-layer, Figure 8c) and rough area (Figure 8d). The tribo-layer was on top of the rough area. The area fraction of the tribo-layer to the total worn surface increased from 10 N (Figure 8a) to 15 N (Figure 8b). Both elements Al and Si were found in the tribo-layer and considered as mechanically mixed layer (EDS result). The rough area was characterized by sharp grains and fine fragments (Figure 8d). The fragments generated from both Al_2O_3 and Si_3N_4 were compacted and sintered at high local pressure and speed.
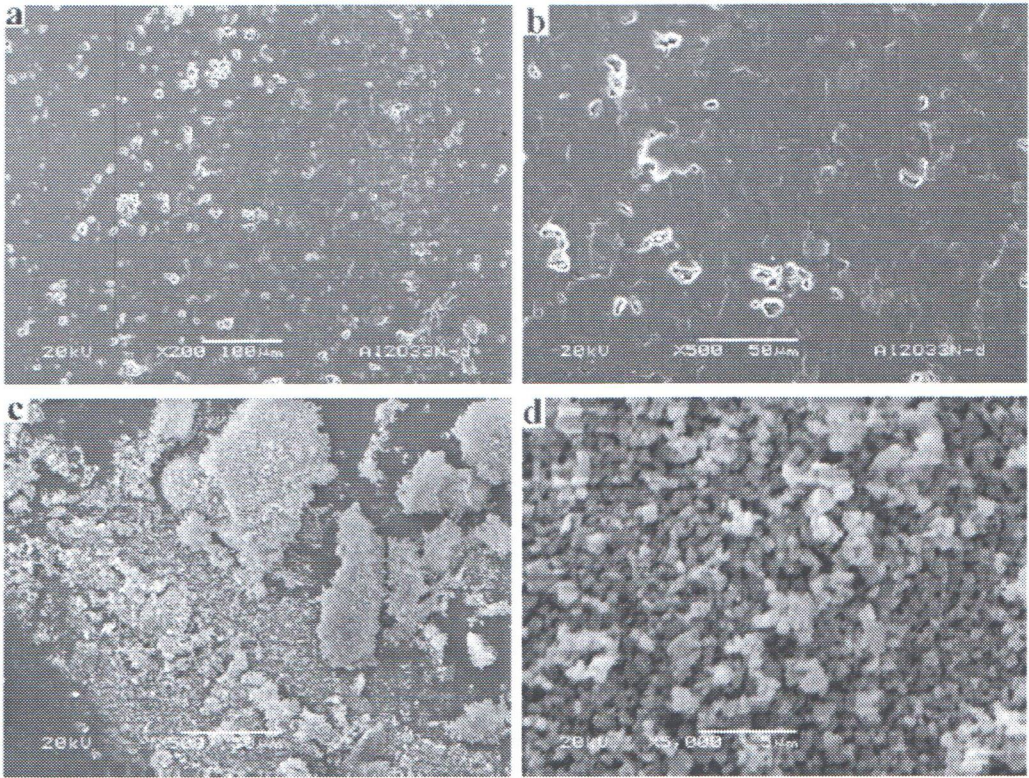
Figure 7. SEM micrographs of (a,b) worn surfaces of monolithic Al$_2$O$_3$ and (c,d) wear debris at 3 N. Black line in Figure 7a is the boundary for wear track and non-wear track.

This might be the formation mechanism of tribo-layer. The detachment of wear debris (plate-like, Figures 8e and 8f) was attributed to the nucleation and propagation of cracks in the tribo-layer (Figure 8c). There were two types of wear debris in Figures 8e and 8f, i.e. fine particles similar to that in Figures 7c and 7d, and large plate-like particles up to several tens of microns. Apparently, the generation of wear debris was time-dependent.

3.3.2. Al$_2$O$_3$-Ni Composite

The worn surface of Al$_2$O$_3$-5%Ni composite at 3 N was very smooth and free of cavities (Figure 9a). For Al$_2$O$_3$-Ni composites, this was the typical characteristic of the worn surfaces under loads of 3 N and 5 N. At 10 N, fracture can be found on the worn surface of Al$_2$O$_3$-5%Ni composites (Figure 9b) and was enhanced at loads of 15 N (Figure 9c) and 20 N (Figure 9d). The critical loads for fractures on the worn surfaces of Al$_2$O$_3$-10%Ni and Al$_2$O$_3$-15%Ni composites were 10 N and 15 N, respectively. Under loads higher than the criticalload, smooth area (Figure 9e) and rough area (Figure 9f) can be found on the worn surface, which was similar to that in Figure 8b. However, the number of cracks in the smooth area in Figure 9e was much less than that in Figure 8b. The typical wear debris at 20 N was plate-like (Figure 10a) and their typical size was several tens of microns, which was much larger than the typical grain size of Al$_2$O$_3$-5%Ni composite. The structure of some wear debris revealed that they were detached by subcritical propagation, Figure 10b.
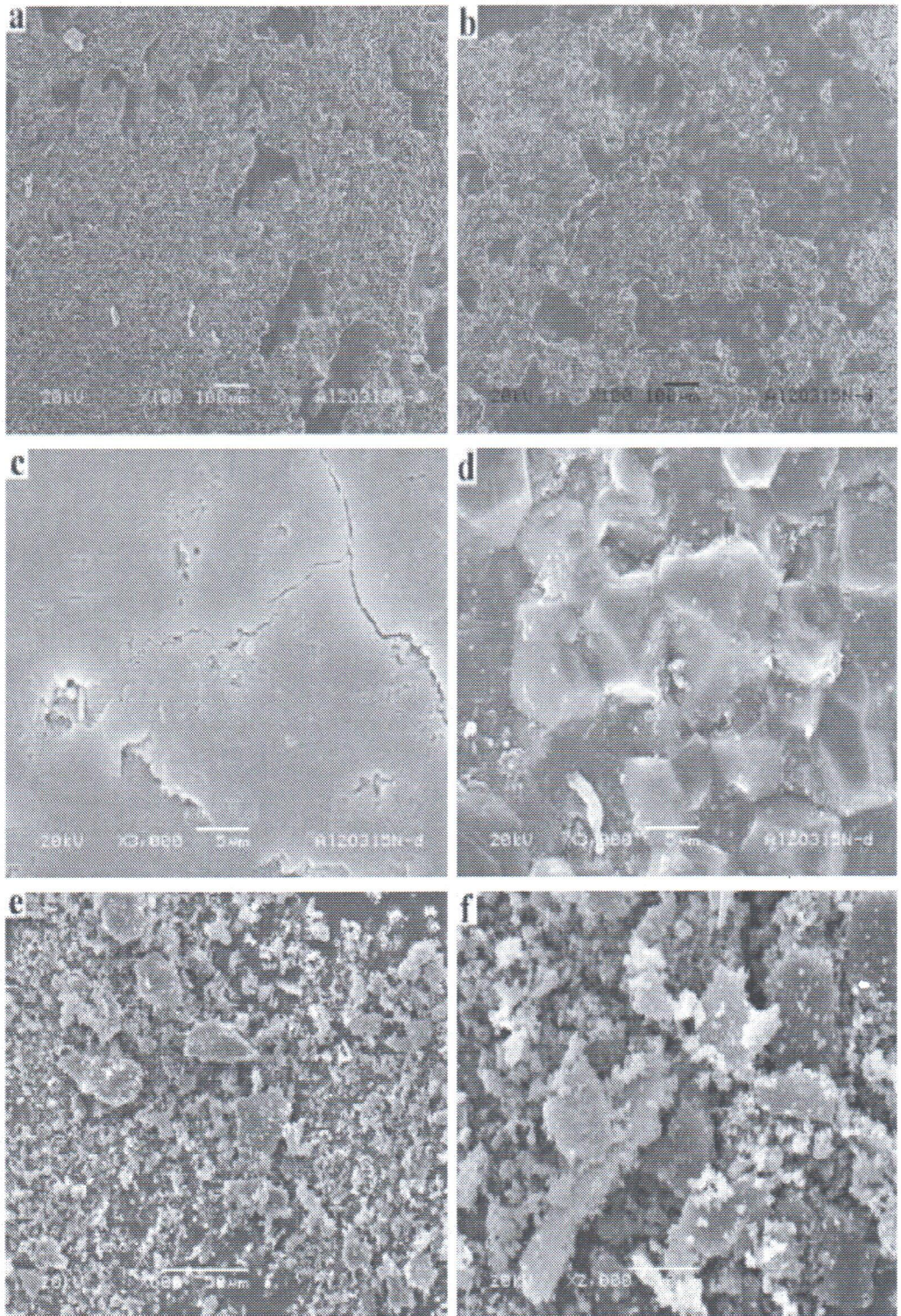
Figure 8. SEM micrographs of worn surfaces of monolithic Al_2O_3 at (a) 10 N, (b,c,d) 15 N and (e,f) wear debris at 15 N.
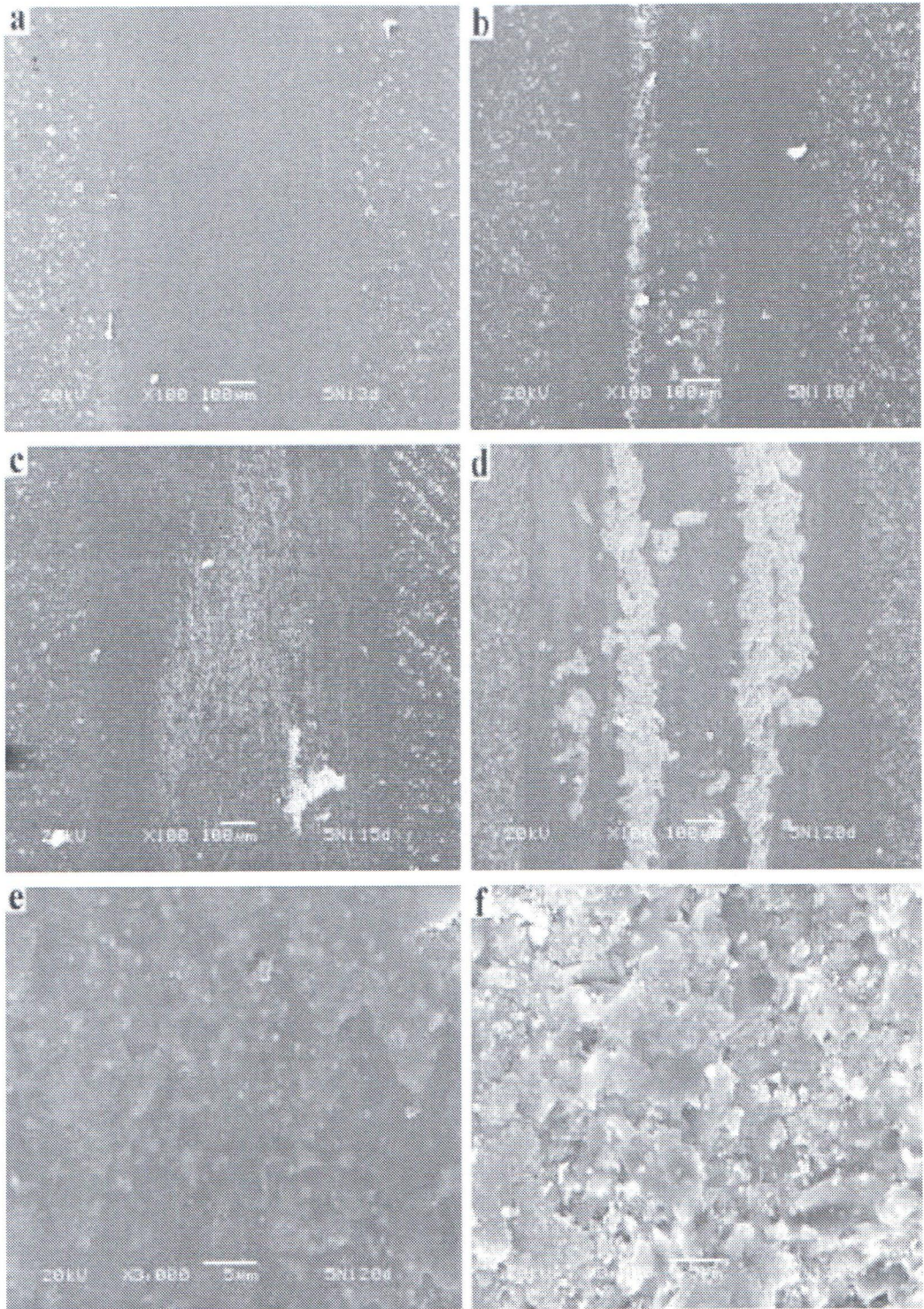
Figure 9. SEM micrographs of worn surfaces of Al$_2$O$_3$-5%Ni composite at (a) 3 N, (b) 10 N, (c) 15 N and (d,e,f) 20 N.
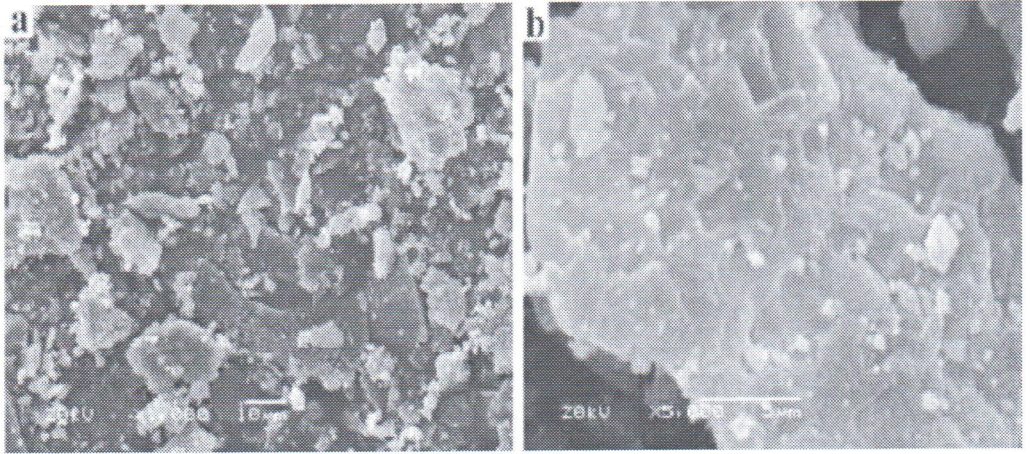
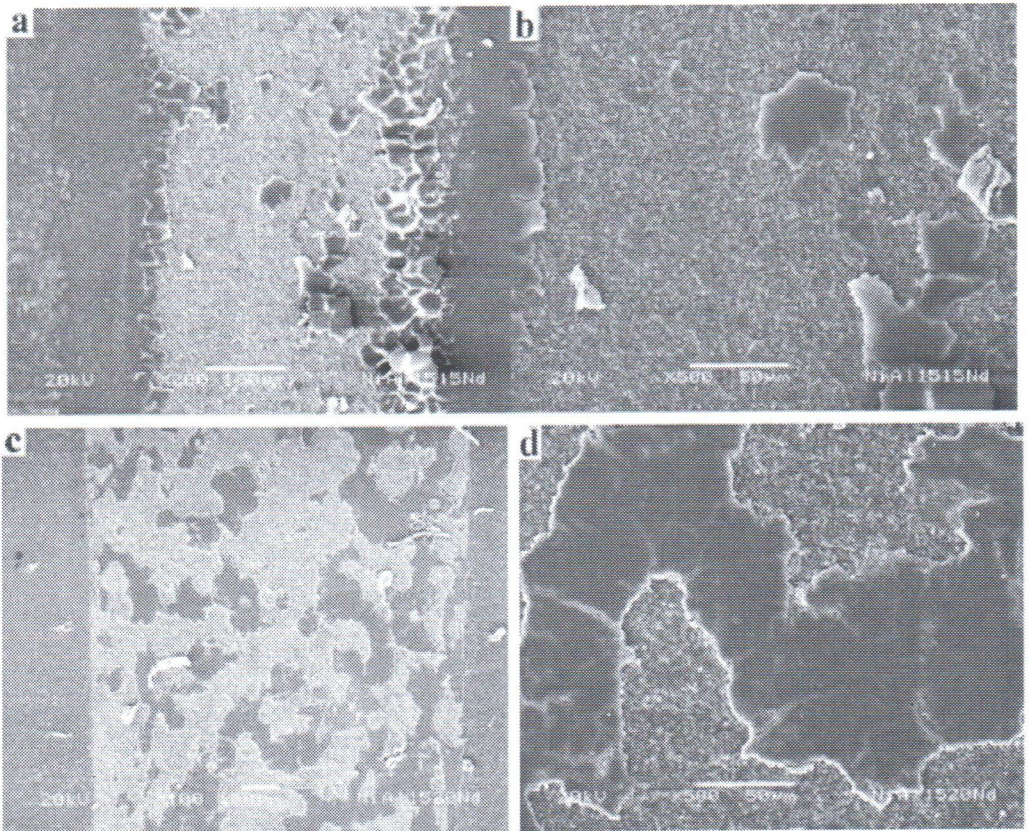Figure 10. SEM micrographs of wear debris of Al_2O_3-5%Ni composite sliding against Si_3N_4 at 20 N.

Figure 11. SEM micrographs of worn surfaces of Al_2O_3-15%Ni composite at (a,b) 15 N and (c,d) 20 N.

It is very interesting that the detachment of tribo-layer on worn surfaces of Al_2O_3-15%Ni composite at 15 N (Figures 11a and 11b) and 20 N (Figures 11c and 11d) were quite different form that in Figures 9b-d. There were many cracks in tribo-layer. Propagation of these cracks resulted in the detachment of tribo-layer.

Wear mechanisms of monolithic Al$_2$O$_3$ and Al$_2$O$_3$-Ni composites in sliding against Si$_3$N$_4$ under high loads were related to formation and failure of tribo-layer. The composition, microstructure, mechanical properties of tribo-layer varied from monolithic Al$_2$O$_3$ to Al$_2$O$_3$-Ni composites. They also depended on content of Ni in the composites. As such, it is understandable that various modes of detachment of tribo-layer in Figures 8, 9 and 11. To reveal the composition, microstructure, mechanical properties of tribo-layer, a lot of work should be done in the future.

CONCLUSION

Microstructure of Al$_2$O$_3$-Ni composites was characterized by inter-type and intra-type of Ni particles in Al$_2$O$_3$ matrix. The addition of Ni resulted in reduced hardness while increased bending strength. A transition from mild wear to severe wear with increased load was found for Al$_2$O$_3$/Si$_3$N$_4$ tribo-couple. There was no such a transition for all Al$_2$O$_3$-Ni composites in sliding against a Si$_3$N$_4$ ball. At high loads, Al$_2$O$_3$-Ni composites exhibited much better wear resistance than that of monolithic Al$_2$O$_3$. The formation and detachment of tribo-layer were the key factors influencing the tribological behavior and wear mechanisms of monolithic Al$_2$O$_3$ and Al$_2$O$_3$-Ni composites.

REFERENCES

[1]   Jahanmir S. *Friction and wear of ceramics*. Marcel Dekker, Inc: New York, US, 1994.
[2]   Tomlinson W.J.; Matthews S.J.; *Ceram. Inter.* 1994, *vol20*, 201-209.
[3]   Hsu S.M.; Shen M. *Wear* 2004, *vol256*, 867-878.
[4]   Adachi K.; Kato K.; Chen N. *Wear* 1997, *vol203-204*, 291-301.
[5]   Pasaribu H.R.; Sloetjes J.W.; Schipper D.J. *Wear* 2003, *vol255*, 699-707.
[6]   Sekino T.; Nakajima T.; Ueda S.; Niihara K. *J. Am. Ceram. Soc.* 1997, *vol80*, 1139-1148.
[7]   Niihara K. *J. Ceram. Soc. Jpn.* 1991, *vol99*, 974-982.
[8]   Chen J.; Rainforth W.M.; Lee W.E. *Scrip. Mater.* 2000, *vol42*, 555-560.
[9]   Portu de G.; Guicciardi S.; Melandri C.; Monteverde F. *Wear* 2007, *vol262*, 1346-1352.
[10] Scheppokat S.; Hannink R.; Janseen R.; Portu de G.; Claussen N. *J. Euro. Ceram. Soc.* 2005, *vol25*, 837-845.